

Improved Properties of Coconut Shell Regenerated Cellulose Biocomposite Films using Butyl Methacrylate

Farah Norain Hahary, Salmah Husseinsyah,* and Marliza Mostapha Zakaria

Butyl methacrylate acid (BMA) was used to enhance the properties of coconut shell (CS) and regenerated cellulose (RC) biocomposite films. The effects of coconut shell content and BMA on the tensile properties, crystallinity index (Crl), thermal properties, and morphology of biocomposite films were investigated. An increase in CS content, up to 3 wt.%, increased the tensile strength and modulus of elasticity, but decreased the elongation at break. The CS-RC biocomposite films treated with BMA exhibited higher tensile strength and modulus of elasticity but lower elongation at break. The crystallinity index (Crl) and thermal stability of CS-RC biocomposite films increased with increasing CS up to 3 wt.%. Treated CS biocomposite films had better thermal stability than untreated CS biocomposite films. The presence of BMA increased the crystallinity of CS regenerated cellulose biocomposite films. Enhancement of the interfacial interaction of CS-RC biocomposite films was revealed by morphological study.

Keywords: Coconut shell; Biocomposite films; Regenerated cellulose; Butyl methacrylate acid

Contact information: Division of Polymer Engineering, School of Materials Engineering, Universiti Malaysia Perlis, 02600 Jejawi, Perlis, Malaysia; *Corresponding author: irsalmah@unimap.edu.my

INTRODUCTION

In recent years, biocomposites that are made from natural renewable resources with features of sustainability, biodegradability, and that are environmentally friendly have received much attention and interest in research and industrial areas. The attention is driven by the growing concern for environmental issues, rising expenses, and gradual depletion of petroleum. One of the ways to curb the dependence on fossil fuels is through the utilisation of biopolymers that are also biocompatible and biodegradable (Haafiz *et al.* 2013; Zhao *et al.* 2014). Currently, the most commercially important bio-based composites have matrices that are based on petrochemical-derived polymers and reinforcements based on a variety of natural cellulosic fibres (Kalka *et al.* 2014).

The main disadvantages of current industrial bio-based composites are their structural or chemical inhomogeneities, poor interfacial adhesion between reinforcement and matrix, and problematic end-of-life disposal of the matrix phase. In recent years, all-cellulose composites (ACCs) have been proposed as green composites that aim to eliminate the chemical incompatibility between matrix and reinforcement phases by utilising cellulose for both components. Consequently, not only do some ACCs exhibit mechanical properties superior to those of cellulose-reinforced thermoplastics, but they are also biodegradable in nature (Duchemin *et al.* 2009; Huber *et al.* 2012; Haafiz *et al.* 2013).

Cellulose is one of the most abundant, renewable biopolymers on earth, with outstanding properties such as high flexibility, biocompatibility, good thermal stability, high mechanical strength, and chemical stability (Flieger *et al.* 2003; Geng *et al.* 2014; Li

et al. 2014; Soheilmoghaddam *et al.* 2014a). However, because of its crystalline form and the hydrogen bonds of cellulose, as well as lignin, which bind the cellulose, it is difficult to process, thus restricting its applications (Feng and Fang 2013). The highly ordered crystalline structure makes it very difficult to dissolve in most conventional solvents (Casas *et al.* 2013; Han *et al.* 2013; Soheilmoghaddam *et al.* 2014b). The ability to disrupt the inter-chain hydrogen bonds of cellulose determines the dissolution efficiency of a solvent (Hameed and Guo 2009; Liu *et al.* 2015). N,N-Dimethylacetamide (DMAc) containing lithium chloride is a very frequently used solvent system in cellulose chemistry (Potthast *et al.* 2002a). This solvent can dissolve cellulose with a molecular weight of more than 10^6 under ambient conditions without severe degradation or other undesirable reactions (Potthast *et al.* 2002b; Ishii *et al.* 2008).

Coconut shell (*Cocos nucifera*) is a non-food hard lignocellulosic material that has outstanding potential as a reinforcement material. Coconut shell makes up approximately 15% to 20% by mass of the coconut itself. It is widely available throughout Asia and in places such as Malaysia, Thailand, Indonesia, and Sri Lanka. The utilisation of cellulose in coconut shell as a substitute polymer for the plastic industry in producing biocomposites might present economic advantages as well as effective ways to curb dependence on fossil fuels, thus helping to preserve the environment (Koay *et al.* 2012; Salmah *et al.* 2012; Saleh *et al.* 2013). However, the presence of hydroxyl groups on the surface of lignocellulosic material allows formation of interfacial bonding. Currently, there are a variety of methods used in the modification of fillers to improve the interfacial adhesion between filler and matrix, such as alkaline treatment, silane treatment, esterification, and use of compatibilisers and other chemical compounds (Chan *et al.* 2013). The purpose of filler incorporated and chemical modification is to produce high strength biodegradable composite films that can be useful for packaging and agriculture application such as mulch film, greenhouse covers, plastic bags, and other packaging materials.

In a previous study, we reported the effect of CS content on properties of regenerated cellulose biocomposite films (Norain *et al.* 2014). The current study aims to investigate the influence of butyl methacrylate (BMA) on the mechanical properties, thermal properties, crystallinity index, and morphology of CS-RC biocomposite films.

EXPERIMENTAL

Materials

Coconut shell (CS) was obtained from a market in Perlis, Malaysia. The CS was cleaned manually, dried, crushed, and ground into powder form. The average particle size of CS was 51 μm , as measured by a Malvern particle size analyser, UK. The DMAc and LiCl were supplied by Merck (Germany) and Acros Organic (Belgium), while microcrystalline cellulose (MCC) and sodium chlorite were supplied by Sigma-Aldrich (USA). Sodium hydroxide (NaOH) and sulphuric acid (H_2SO_4) were supplied by HmbG Chemicals (Germany). Glacial acetic acid was provided by BASF (Germany). Butyl methacrylate (BMA) was purchased from Merck (Germany).

Coconut Shell Pretreatment

Coconut shell (CS) with average size of 63 μm was pretreated with the alkali treatment using 4% (w/v) sodium hydroxide solution at 70 °C for 3 h; pretreatment of coconut shell was conducted three times under mechanical stirring. Bleaching treatment

was conducted with a solution containing equal parts acetate buffer (sodium hydroxide, glacial acetic acid, and sodium chlorite) at 70 °C for 1 h under mechanical stirring and was repeated eight times. Acid hydrolysis with 65% sulphuric acid was conducted at 45 °C for 1 h. Cold water was used to dilute the solution after the acid hydrolysis process to stop the reaction. CS was washed, filtered, and dried in oven at 80 °C for 24 h.

Chemical Modification of CS

BMA was dissolved into ethanol (3% (v/v)). The CS was transferred slowly into the BMA solution, stirred for 1 h, and kept overnight. The treated CS was filtered and dried in an oven at 80 °C for 24 h.

Preparation of CS-RC Biocomposite Films

Before dissolution in DMAc could take place, celluloses (MCC and CS) required activation. They were therefore immersed in distilled water, acetone, and DMAc each in succession for 1 h at room temperature. An 8% (w/v) solution of LiCl was used in the cellulose dissolution. The celluloses and LiCl/DMAc mixture was stirred for 1 h until a transparent viscous solution was obtained, which was then cast on to a glass plate, and kept overnight for regeneration to occur. Regenerated cellulose biocomposite films were washed with distilled water. The biocomposite films were dried at room temperature for 24 h. The formulations of CS-RC biocomposite films with various filler contents are shown in Table 1.

Table 1. Formulation of Untreated and Treated CS-RC Biocomposite Films

Materials	Untreated CS-RC biocomposite films	Treated CS-RC biocomposite films
MCC (wt.%)	3	3
CS (wt.%)	1, 2, 3, 4	1, 2, 3, 4
Butyl methacrylate acid (%) ^a	-	3

^a3% based on weight of CS

X-Ray Diffraction (XRD)

The crystallinity index (CrI) of RC biocomposite films was determined using a Bruker D8Advance, USA. The pattern with Cu K α 1 ($\lambda=1.5406 \text{ \AA}$) was generated at 30 kV and 10 mA. The crystallinity index (CrI) was calculated using the Segal method, given by Eq. 1,

$$\text{CrI (\%)} = (I_{002} - I_{AM}) / I_{002} \times 100 \quad (1)$$

where I_{002} is the height of the (002) lattice diffraction peak, which represents both crystalline and amorphous material, and I_{AM} is the lowest height between the 200 and 110 peaks, which represents amorphous material only.

Tensile Testing

Tensile properties such as tensile strength, modulus of elasticity, and elongation at break can be obtained from tensile tests. Tensile testing of RC biocomposite films was conducted using an Instron Universal Testing Machine, Model 5569, USA. A cross-head speed of 10 mm/min was used, and the test was carried out at room temperature. Five samples with sizes of 50 x 15 mm, cut from each of the RC biocomposite films, were tested.

The statistical analysis for T-test analysis was performed using JMP Pro 12 to determine the level of significant between untreated and treated biocomposite films with respect to tensile strength and modulus of elasticity data.

Morphology Analysis

The morphological study of the tensile fracture surface of CS-RC biocomposite films was carried out using a scanning electron microscope (SEM), model JEOL JSM-6460 LA (USA) at an accelerating voltage of 15 kV. The fractured ends of tensile specimens were mounted on aluminum stubs and sputter coated with thin layer of palladium to avoid electrostatic charging during examination.

Thermogravimetric Analysis (TGA)

The thermal properties of CS-RC biocomposite films were characterised using a TGA Pyris Diamond (Perkin-Elmer), Germany. The temperature was varied from 30 to 600 °C with heating rate of 10 °C/min under a nitrogen atmosphere. A nitrogen flow of 50 mL/min was used for this test.

Fourier Transmission Infrared Spectroscopy (FTIR)

FTIR-analysis was used to characterise the presence of the functional chemical groups in untreated and treated CS-RC biocomposite films. The FTIR analysis was carried out using a Perkin Elmer, Model L1280044 (Germany). The attenuated total reflectance (ATR) method was used. Sixteen scans were recorded per sample in the frequency range of 4000 to 400 cm^{-1} with a resolution of 4 cm^{-1} .

RESULTS AND DISCUSSION

X-Ray Diffraction

The XRD patterns of untreated and CS-RC biocomposite films treated with BMA are shown in Fig. 1. Table 2 shows the crystallinity index (CrI) of CS-RC biocomposite films with various CS contents. The diffractogram of CS-RC biocomposite films shows characteristic peaks at approximately $2\theta = 11^\circ$ to 12° , which corresponds to the (110) plane, whereas those at approximately $2\theta = 20^\circ$ and $2\theta = 22^\circ$ correspond to the (110) and (020) planes, respectively. These three peaks are characteristic of regenerated cellulose films. The crystalline structure partially remained in the regenerated cellulose, which was caused by the cleavage of the inter- and intra-molecular hydrogen bonds of cellulose during the process of dissolution and the partial reconstitution of the hydrogen bond network of the regenerated cellulose during the course of precipitation. As can be seen from Table 2, the crystallinity index (CrI) of untreated CS-RC biocomposite films increased proportionally with CS content up to 3 wt.%. Further increments of CS contents resulted in a decrease in the crystallinity of cellulose biocomposite films. This could be due to poor dissolution at higher CS content, which induced the reduction of the CrI value. Duchemin *et al.* (2009) reported that the concentration of cellulose used for dissolution at a given dissolution time affects the crystallinity of cellulose. Treated CS-RC biocomposite films with BMA exhibited higher crystallinity at 3 wt.% of CS than the untreated CS-RC biocomposite films. This is because of a strong interaction between the hydrogen bonds of CS and the regenerated cellulose matrix, which exhibited formation during the dissolution phase, thus increasing the crystallinity of biocomposite films.

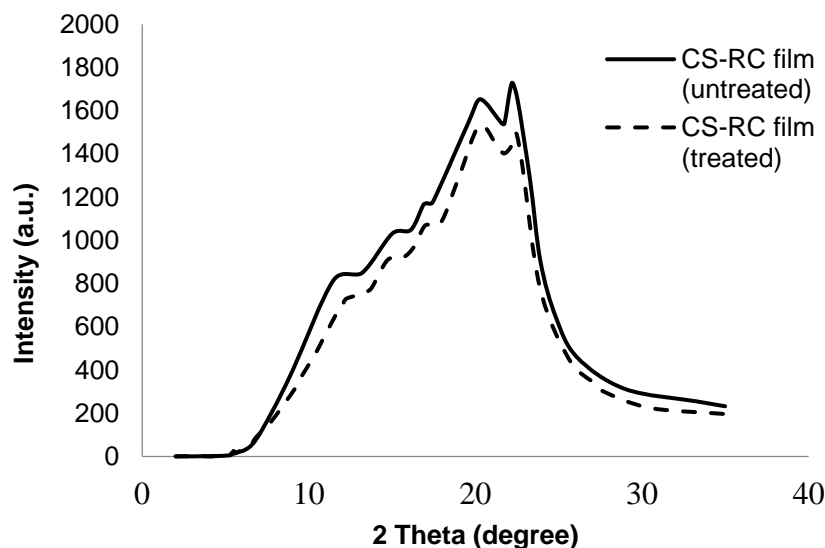


Fig. 1. XRD curves of untreated and treated CS-RC biocomposite film with BMA at 3 wt.% of CS.

Table 2. Crystallinity Index (Crl) of Untreated and Treated CS-RC Biocomposite Films with BMA

CS-RC biocomposite films	Crystallinity index (Crl) (%)	
	Untreated CS-RC	Treated CS-RC
CS-RC films 0 wt.%	52.4	-
CS-RC films 1 wt.%	52.8	54.4
CS-RC films 2 wt.%	53.8	55.9
CS-RC films 3 wt.%	55.5	57.7
CS-RC films 4 wt.%	49.7	50.4

Tensile Properties

Figure 2 shows the effect of CS content on the tensile strength of untreated and treated CS regenerated cellulose biocomposite films. As the CS content increased, the tensile strength of the regenerated cellulose films also increased, up to 3 wt.%. The improvement in tensile strength, especially at 3 wt.%, may be due to various factors affecting the coherence between the regenerated cellulose matrix and CS particles. As the CS content further increased, the tensile strength decreased. The increase in CS content caused a decrement in mechanical performance compared to lower concentrations because of poor dispersion in the matrix, thus resulting in the formation of agglomerates between celluloses in CS-RC biocomposites films. The presence of high CS content also caused stress concentration at the filler surface. The CS-RC biocomposite films treated with BMA showed higher tensile strength than the untreated CS-RC biocomposite films. This is because the BMA improved the filler-matrix interaction, thus promoting strong interactions with the cellulose matrix through hydrogen bonds. It was also found that 3 wt.% CS led to an improvement in the tensile strength for CS-RC biocomposite films treated with BMA. T-test analysis for tensile strength showed that $\text{Prob} > t$ for untreated-treated was greater than $\alpha=0.05$ indicated that there is a significant difference between untreated and treated CS RC biocomposite films. The analysis result showed that the tensile strength treated $>$ untreated biocomposite films.

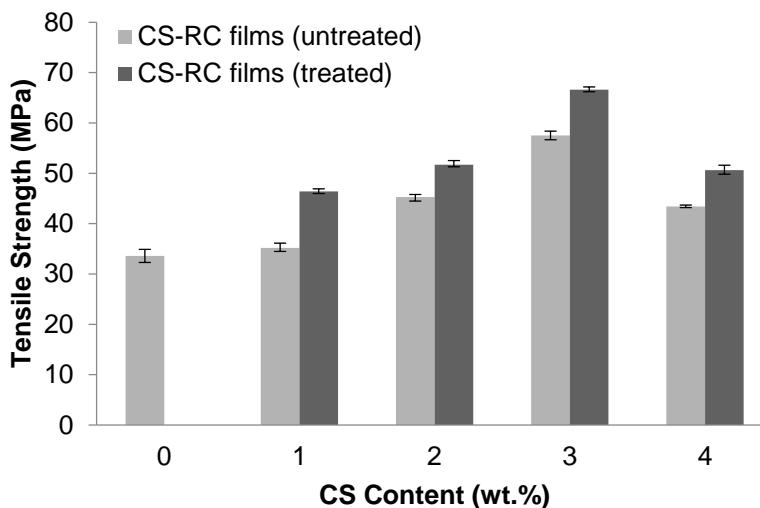


Fig. 2. The effect of CS content on the tensile strength of untreated and treated CS-RC biocomposites films

Figure 3 shows the effect of CS contents on elongation at break of untreated and treated CS-RC biocomposite films. The elongation at break of CS-RC biocomposite films decreased as the CS content increased for both untreated and treated CS-RC biocomposite films up to 3 wt.%. This could be attributed to the presence of CS, which restrains the slippage movement of regenerated cellulose biocomposite film chains during deformation, resulting in decreased elongation at break values for the untreated CS-RC biocomposite films. At higher CS contents, the domination of filler-matrix interactions can be expected to subside and be substituted by filler-filler interactions. Nevertheless, the treated CS-RC biocomposite films exhibit lower elongation at break at 3 wt.% of CS compared to the untreated CS-RC biocomposite films. The treatment with BMA improves the stiffness of the biocomposite films because of strong interactions between CS and the RC matrix.

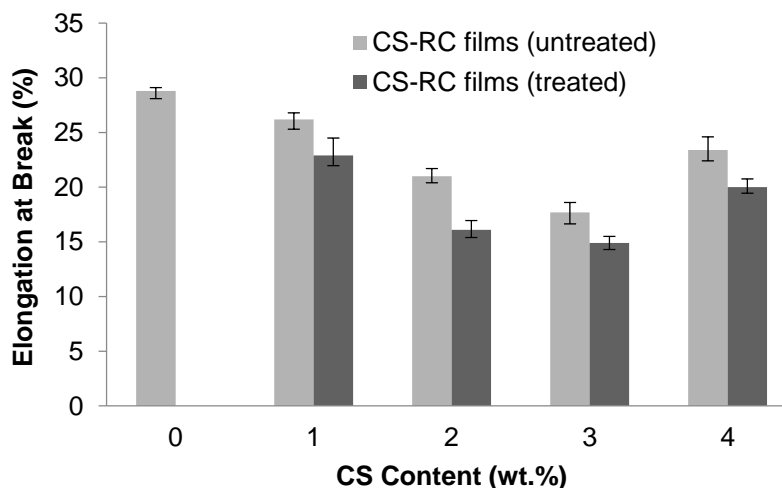


Fig. 3. The effect of CS content on elongation at break of untreated and treated CS-RC biocomposite films

Figure 4 illustrates the effect of CS content on the modulus of elasticity of both untreated and treated CS-RC biocomposite films. The modulus of elasticity of CS-RC

biocomposite films increased linearly up to 3 wt.% CS, but as the CS content further increased to 4 wt.%, the modulus of elasticity decreased, which can be attributed to a reduced level of dispersion for untreated CS-RC biocomposite films. At similar CS contents, treated CS-RC biocomposite films exhibited a higher modulus of elasticity than the untreated CS-RC biocomposite films. This is because of a rigidity of CS that led to a reduction in deformation capabilities and therefore suppressed the cellulose movement of biocomposite films. Modulus of elasticity from the t-test analysis show that $\text{Prob} > t$ for untreated-treated was greater than $\alpha=0.05$ indicating a significant difference between untreated and treated CS RC biocomposite films. Based on the t-test analysis result, we conclude that treated > untreated biocomposite films.

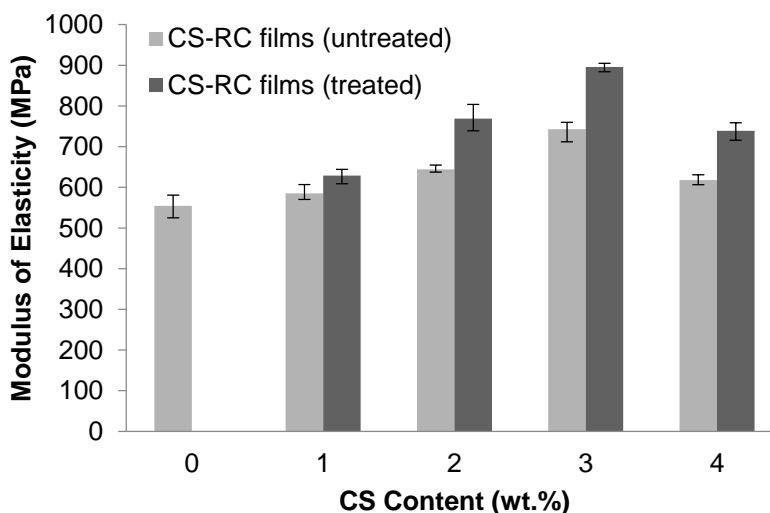


Fig. 4. The effect of CS contents on the modulus of elasticity of untreated and treated CS-RC biocomposites films

Morphology Study

A scanning electron microscope (SEM) was used to examine the tensile fracture surface of the CS-RC biocomposite films at 1 and 3 wt.% CS contents, as shown in Figs. 5a) to 5d). The SEM micrographs of untreated CS-RC biocomposite films are shown in Figs. 5a) and b), respectively. The micrographs of untreated CS-RC biocomposite films show rough surfaces for 1 wt.% CS content, which indicates formation of agglomeration and voids in biocomposite films. At 3 wt.%, the micrograph showed a less rough surface, with fewer voids, as shown in Fig. 5b). The results indicate good interfacial interaction between the regenerated cellulose matrix and CS. Figs. 5c) and d) show SEM micrographs of the tensile surface fracture of CS-RC biocomposite films treated with BMA at CS contents of 1 and 3 wt.%, respectively. The treated CS-RC biocomposite films show a smoother surface fracture than the untreated biocomposite films. This is because of better interfacial adhesion between treated CS in RC biocomposite films. The better interfacial bonding was also reflected in the improvement of the tensile properties of the treated biocomposite films.

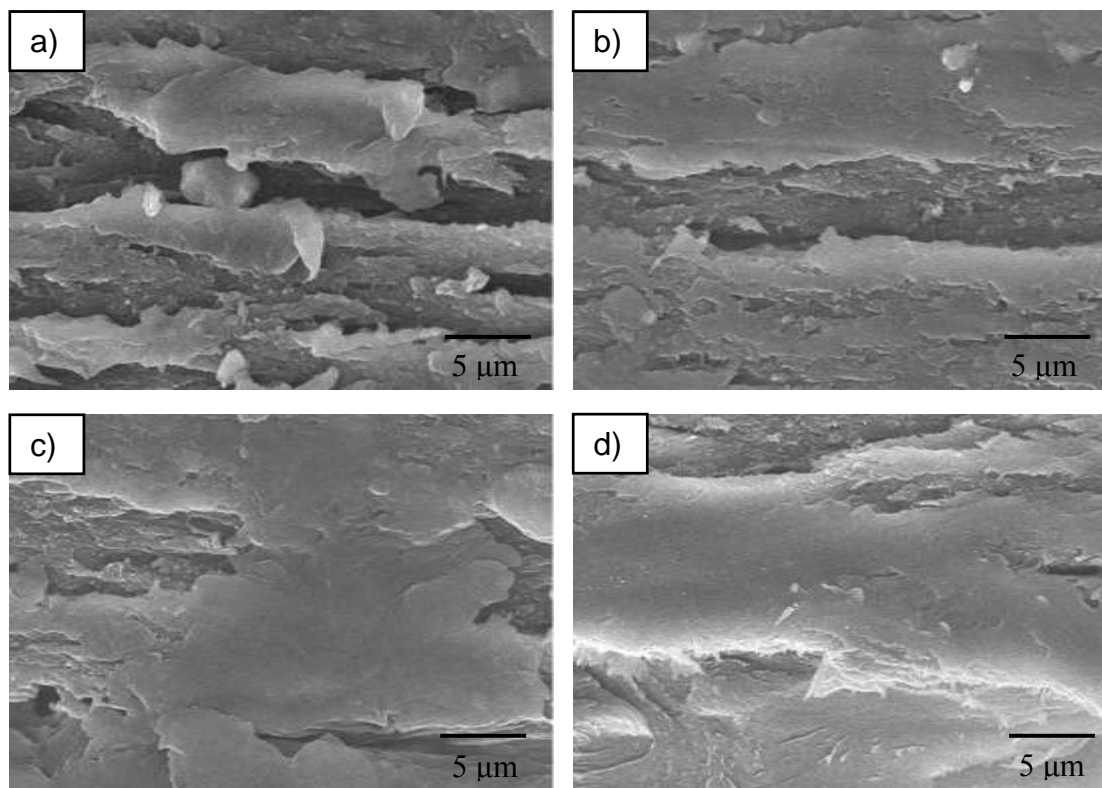


Fig. 5. SEM micrograph of fracture surface: (a) untreated CS-RC films (1 wt.%); (b) untreated CS-RC films (3 wt.%); (c) treated CS-RC films (1 wt.%); (d) treated CS-RC films (3 wt.%)

Thermogravimetric Analysis

Results of the thermogravimetric analysis of untreated and treated CS-RC biocomposite films at various CS contents are shown in Fig. 6. Table 3 summarises the data from the TGA curves. As can be seen, cellulose displayed two weight loss stages. All regenerated cellulose samples exhibited weight loss at 100 °C as a result of the evaporation of the absorbed water in cellulose.

The data reveal that CS contents had a marked effect on the thermal stability of biocomposite films. The total weight loss of untreated CS-RC biocomposite films with CS content of 3 wt.% was lower than those with 1 wt.%, which indicates that incorporation of higher CS contents enhanced the thermal stability of the RC biocomposite films. This may be because CS could hinder the diffusion of heat mass transfer to the surface, thus retarding the decomposition rate.

The weight loss of untreated RC biocomposite films at 300 and 600 °C decreased with increasing CS content. The lower weight loss indicated better thermal stability, attributed to char formation during the pyrolysis of CS, which acts as a protective layer that suppresses the thermal decomposition of biocomposite films. At similar CS contents, the weight loss of treated biocomposite films at 300 and 600 °C are lower than those of the untreated biocomposite films. Meanwhile, char residue increased with increasing CS contents. The improvement in thermal stability of the treated biocomposite films was attributed to the strong interaction between the CS and RC matrix, which contributed to the formation of a char layer as a thermal protection.

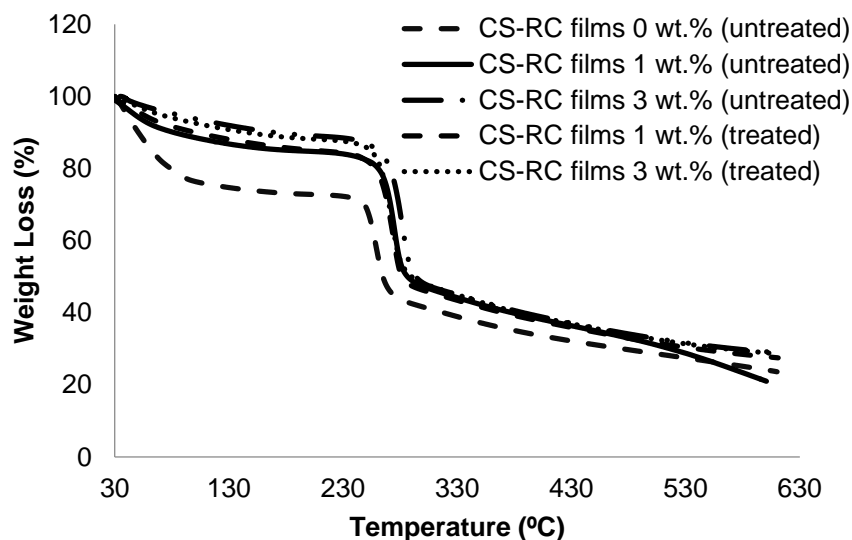


Fig. 6. TGA curves of untreated and treated CS-RC biocomposites films with BMA at different CS content.

Table 3. TGA Data of Untreated and Treated CS-RC Biocomposite Films with BMA

CS-RC biocomposite films (wt.%)	T_{dmax} (°C)	Weight loss (%)		Char Residue (%)
		300 °C	600 °C	
CS-RC films 0 wt.% (Untreated)	258	58.40	75.81	24.19
CS-RC films 1 wt.% (Untreated)	274	52.67	78.90	21.01
CS-RC films 3 wt.% (Untreated)	281	51.71	70.79	28.93
CS-RC films 1 wt.% (Treated)	276	52.18	69.97	29.85
CS-RC films 3 wt.% (Treated)	278	50.63	67.73	31.12

Fourier Transform Infrared Spectroscopy Analysis

The FTIR spectra of untreated CS-RC biocomposites and those treated with butyl methacrylate acid (BMA) are shown in Fig. 7. The broad band in the 3389 cm^{-1} region for untreated CS-RC biocomposite films is due to the OH- stretching vibration in cellulose. The peak at 2910 cm^{-1} is related to the C-H stretching of untreated biocomposite films. The adsorption at 1644 cm^{-1} is due to C=O stretching of carbonyl from the hemicelluloses. The intensity peak at 1361 cm^{-1} is attributed to the CH_2 bonding vibration. The peaks at 1052 and 1024 cm^{-1} represent stretching of C-O-C groups in cellulose. The FTIR absorption band at 894 cm^{-1} is assigned to C-O stretching at the β -(1-4)-glycosidic linkage, which indicates an amorphous absorption band of cellulose in CS RC biocomposite films. Buty methacrylate improved the properties of the biocomposite films by reduced intensity of the hydroxyl group (-OH) from 3389 to 3374 cm^{-1} , which is due to the reaction of BMA with the -OH group on the CS surface. This suggests that the hydrophilic nature of CS was reduced by the reaction. The peak at 2296 cm^{-1} was reduced in treated RC biocomposites, indicating a change in the conformation of CH_2OH at the C_6 position. The reduced peak at 1644 to 1638 cm^{-1} is due to the OH-bending of adsorbed water. The intensity at 1376 cm^{-1} increased because of the C-H bending vibration in treated CS-RC biocomposite films.

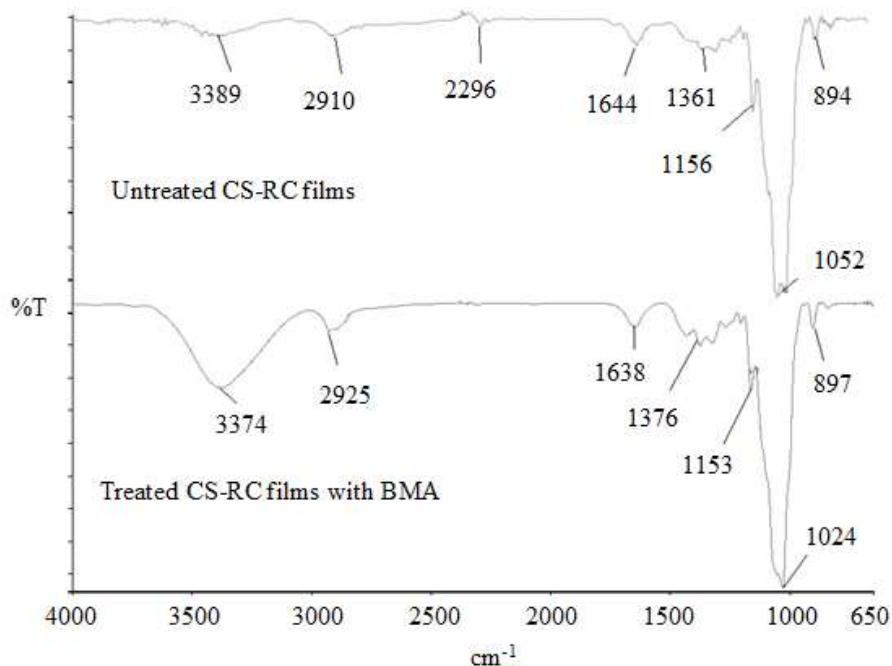


Fig. 7. FTIR spectra of untreated and treated CS-RC biocomposite films with BMA

Figure 8 shows a schematic of the reaction between CS and BMA.

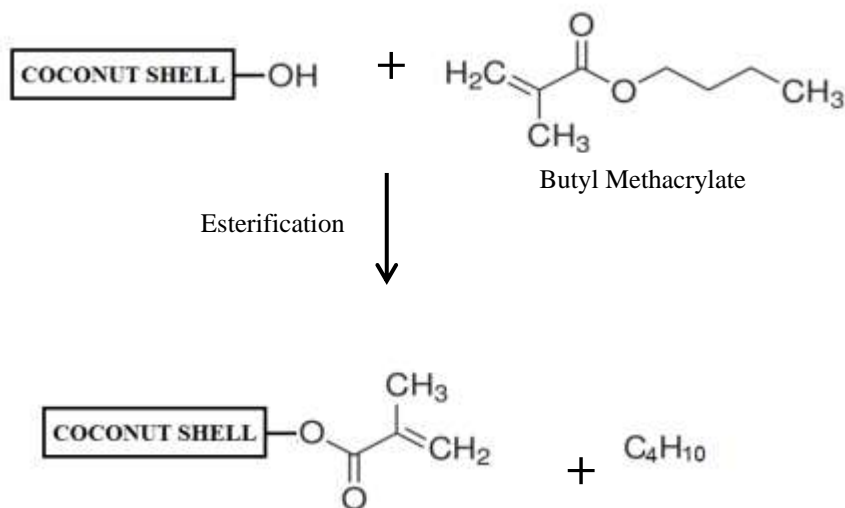


Fig. 8. The schematic reaction of CS with BMA

CONCLUSIONS

1. The tensile strength and modulus of elasticity of RC biocomposite films increased as coconut shell (CS) was added at up to 3 wt.% by mass and decreased at higher contents of CS. The elongation at break decreased with increasing CS content and increased at 4 wt.% CS.

2. The crystallinity index (CrI) and thermal stability also increased up to 3 wt.% and decreased at higher CS contents.
3. The morphology study showed that at 3 wt.% of CS there was better interaction between CS in the RC biocomposite films.
4. Treatment with BMA enhanced the tensile strength, modulus of elasticity, crystallinity index (CrI), and thermal stability of biocomposite films.
5. Treatment with BMA improved the interfacial interaction and dispersion of CS particles in the CS-RC matrix.

ACKNOWLEDGMENTS

The authors are grateful for the support from the Ministry of Education (MOE). Special thanks to the Fundamental Research Grant Scheme (FRGS), Phase-2, 2013 for financial support.

REFERENCES CITED

- Casas, A., Alonso, M. V., Oliet, M., Santos, T. M., and Rodriguez, F. (2013). "Characterization of cellulose regenerated from solutions of pine and eucalyptus woods in 1-allyl-3-methylimidazolium chloride," *Carbohydr. Polym.* 92(2), 1946-1952. DOI: 10.1016/j.carbpol.2012.11.057
- Chan, M. Y., Salmah H., and Sam, S. T. (2013). "Modified corn cob filled chitosan biocomposite films," *Polym. Plast. Technol. Eng.* 52(14), 1496-1502. DOI: 10.1080/03602559.2013.820752
- Duchemin, B. J. C., Newman, R. H., and Staiger, M. P. (2009). "Structure-property relationship of all-cellulose composites," *Compo. Sci. Technol.* 69(7-8), 1225-1230. DOI: 10.1016/j.compscitech.2009.02.027
- Feng, G., and Fang, Z. (2013). "Solid- and nano-catalysts pretreatment and hydrolysis techniques," in: *Pretreatment Techniques for Biofuels and Biorefineries*, Z. Fang (ed.), Springer, Berlin, pp. 339-366. DOI: 10.1007/978-3-642-32735-3_15
- Flieger, M., Kantorova, M., Prell, A., Rezanka, T., and Votruba, J. (2003). "Biodegradable plastics from renewable sources," *Folia Microbiol.* 48(1), 27-44. DOI: 10.1007/BF02931273
- Geng, H., Yuan, Z., Fan, Q., Dai, X., Zhao, Y., Wang, Z., and Qin, M. (2014). "Characterisation of cellulose films regenerated from acetone/water coagulants," *Carbohydr. Polym.* 102, 438-444. DOI: 10.1016/j.carbpol.2013.11.071
- Haafiz, M. K. M., Hassan, A., Zakaria, Z., Inuwa, I. M., Islam, M. S., and Jawaid, M. (2013). "Properties of polylactic acid composites reinforced with oil palm biomass microcrystalline cellulose," *Carbohydr. Polym.* 98(1), 139-145. DOI: 10.1016/j.carbpol.2013.05.069
- Hameed, N., and Guo, Q. (2009). "Natural wool/cellulose acetate blends regenerated from the ionic liquid 1-butyl-3-methylimidazolium chloride," *Carbohydr. Polym.* 78(4), 999-1004. DOI: 10.1016/j.carbpol.2009.07.033

- Han, J., Zhou, C., French, A. D., Han, G., and Wu, Q. (2013). "Characterization of cellulose II nanoparticles regenerated from 1-butyl-3-methylimidazolium chloride," *Carbohydr. Polym.* 94(2), 773-781. DOI: 10.1016/j.carbpol.2013.02.003
- Huber, T., Mussig, J., Curnow, O., Pang, S., Bickerton, S., and Staiger, M. P. (2012). "A critical review of all-cellulose composites," *J. Mater. Sci.* 47(3), 1171-1186. DOI: 10.1007/s10853-011-5774-3
- Ishii, D., Tatsumi, D., and Matsumoto, T. (2008). "Effect of solvent exchange on the supramolecular structure, the molecular mobility and the dissolution behavior of cellulose in LiCl/DMAc," *Carbohydr. Res.* 343(5), 919-928. DOI: 10.1016/j.carres.2008.01.035
- Kalka, S., Huber, T., Steinberg, J., Baronian, K., Mussig, J., and Staiger, M. P. (2014). "Biodegradability of all-cellulose composite laminates," *Composites Part A* 59, 37-44. DOI: 10.1016/j.compositesa.2013.12.012
- Koay, S. C., Salmah, H., and Hakimah, O. (2012). "Properties of coconut shell powder-filled polylactic acid ecomposites: Effect of maleic acid," *Polym. Eng. Sci.* 53(5), 1109-1116. DOI: 10.1002/pen.23359
- Li, C., Liu, Q., Shu, S., Xie, Y., Zhao, Y., Chen, B., and Dong, W. (2014). "Preparation and characterization of regenerated cellulose/TiO₂/ZnO nanocomposites and its photocatalytic activity," *Mater. Lett.* 117, 234-236. DOI: 10.1016/j.matlet.2013.12.009
- Liu, Z., Sun, X., Hao, M., Huang, C., Xue, Z., and Mu, T. (2015). "Preparation and characterization of regenerated cellulose from ionic liquid using different methods," *Carbohydr. Polym.* 117, 99-105. DOI: 10.1016/j.carbpol.2014.09.053
- Norain H. F., Salmah H., and Marliza, M. (2015). "Properties of all-cellulose composite films from coconut shell powder and microcrystalline cellulose," *App. Mech. Mater.* 754-755, 39-43. DOI: 10.4028/www.scientific.net/AMM.754-755.39
- Potthast, A., Rosenau, T., Buchner, R., Roder, T., Ebner, G., Bruglachner, H., Sixta, H., and Kosma, P. (2002a). "The cellulose solvent system N,N-dimethylacetamide/lithium chloride revisited: The effect of water on physicochemical properties and chemical stability," *Cellulose* 9(1), 41-53. DOI: 10.1023/A:1015811712657
- Potthast, A., Rosenau, T., Sixta, H., and Kosma, P. (2002b). "Degradation of cellulosic materials by heating in DMAc/LiCl," *Tetrahedron Lett.* 43(43), 7757-7759. DOI: 10.1016/S0040-4039(02)01767-7
- Saleh, Z., Islam, M. M., and Ku, H. (2013). "Tensile behaviours of activated carbon coconut shell filled epoxy composites," *3rd Malaysia Postgraduate Conference (MPC2013)*, 22-27.
- Salmah, H., Koay S. C., and Hakimah, O. (2012). "Surface modification of coconut shell powder filled polylactic acid biocomposites," *J. Thermoplast. Compos. Mater.* 26(6), 809-819. DOI: 10.1177/0892705711429981
- Segal, L., Creely, J. J., Martin Jr, A. E., and Conrad, M. C. (1959). "An empirical method for estimating the degree of crystallinity of native cellulose using the X-ray diffractometer," *Text. Res. J.* 29(10), 786-94. DOI: 10.1177/004051755902901003
- Soheilmoghaddam, M., Pasbakhsh, P., Wahit, M. U., Bidsorkhi, H. C., Pour, R. H., Whye, W. T., and De Silva, R. T. (2014a). "Regenerated cellulose nanocomposites reinforced with exfoliated graphite nanosheets using BMIMCL ionic liquid," *Polymer* 55(14), 3130-3138. DOI: 10.1016/j.polymer.2014.05.021

Soheilmoghaddam, M., Sharifzadeh, G., Pour, R. H., Wahit, M. U., Whye, W. T., and Lee, X. Y. (2014b). "Regenerated cellulose/ β -cyclodextrin scaffold prepared using ionic liquid," *Mater. Lett.* 135, 210-213. DOI: 10.1016/j.matlet.2014.07.169

Zhao, J., He, X., Wang, Y., Zhang, W., Zhang, X., Zhang, X., Deng Y., and Lu, C. (2014). "Reinforcement of all-cellulose nanocomposite films using native cellulose nanofibrils," *Carbohydr. Polym.* 104, 143-150. DOI: 10.1016/j.carbpol.2014.01.007

Article submitted: August 19, 2015; Peer review completed: October 16, 2015; Revised version received and accepted: November 12, 2015; Published: November 30, 2015.
DOI: 10.15376/biores.11.1.886-898